

Electronic Supplementary Information

Selective transformation of carbon dioxide into lower olefins with a bifunctional catalyst composed of ZnGa₂O₄ and SAPO-34

Xiaoliang Liu, Mengheng Wang, Cheng Zhou, Wei Zhou, Kang Cheng,* Jincan Kang,
Qinghong Zhang,* Weiping Deng and Ye Wang*

*State Key Laboratory of Physical Chemistry of Solid Surfaces, Collaborative Innovation Center of
Chemistry for Energy Materials, National Engineering Laboratory for Green Chemical
Productions of Alcohols, Ethers and Esters, College of Chemistry and Chemical Engineering,
Xiamen University, Xiamen 361005, P. R. China.*

Experimental Details

Materials and catalyst preparation

The Zn–Ga–O oxides were synthesized by a co-precipitation method. Typically, Ga(NO₃)₃·xH₂O (M = 255.5 g mol⁻¹) and Zn(NO₃)₂·6H₂O with a fixed molar ratio were dissolved into 100 mL deionized water. Then, an aqueous ammonia solution (25 wt%) was added dropwise into the mixed solution at room temperature until the pH reached 7.0. The obtained white precipitate was aged for 2 h at 70 °C. The solid product was recovered by filtration, followed by washing with deionized water and drying in air at 100 °C for 12 h. After calcination in air at 500 °C for 5 h, the obtained catalyst was denoted as Zn–Ga–O (*m:n*), where *m:n* is the molar ratio of Zn/Ga. Typically, the Zn–Ga–O catalyst with a Zn/Ga molar ratio of 1:2 was used for

discussion unless otherwise mentioned.

For comparison, a Cu–Zn–Al (Cu/Zn/Al = 6:3:1, molar ratio) mixed oxide was also prepared by the co-precipitation method. Briefly, Na₂CO₃ aqueous solution was added into mixed solution of metal nitrates [Cu(NO₃)₂·3H₂O (0.6 M), Zn(NO₃)₂·6H₂O (0.3 M) and Al(NO₃)₃·9H₂O (0.1 M)] under continuous stirring at a temperature of 70 °C and a constant pH of 7.0. The suspension was aged for 2 h at the same temperature. The solid product was recovered by filtration, followed by washing with deionized water, drying in an oven at 100 °C for 12 h, and finally calcination in air flow at 300 °C for 3 h.

SAPO-34 was synthesized by a hydrothermal method from a gel with a molar composition of TEA/Al₂O₃/SiO₂/P₂O₅/H₂O = 3:1:0.25:1:50.¹ Pseudoboehmite (72 wt% Al₂O₃), orthophosphoric acid (85 wt% H₃PO₄), silica sol (30 wt% SiO₂) and triethylamine (TEA) were used as the source materials. Pseudoboehmite (4.7 g) was dissolved in 50 mL deionized water to form alumina sol, and then silica sol (1.5 g) was added to the alumina sol under stirring for 2 h. Trimethylamine (11.3 g) was then added slowly under continual stirring for another 2 h. After that, orthophosphoric acid (7.3 g) was added to the mixture, and stirred for 12 h until a homogeneous gel mixture was obtained. The gel mixture was sealed in a 200 mL Teflon-lined stainless-steel vessel and was heated from room temperature to 200 °C at a rate of 2 °C min⁻¹. The crystallization was carried out at 200 °C under autogenic pressure for 72 h. After crystallization, the as-synthesized sample was obtained by centrifugation, washing, and drying at 100 °C for 6 h. Finally, the sample was calcined at 550 °C for 6 h to remove the organic template.

The bifunctional catalyst was prepared by a simple mortar-mixing method. The weight ratio of the Zn–Ga–O and SAPO-34 was fixed at 1:2. Briefly, the Zn–Ga–O sample and the SAPO-34 were manually mixed in an agate mortar for 10 min. The obtained catalyst was denoted as Zn–Ga–O/SAPO-34.

Catalytic reaction

The catalytic reaction was performed with a high-pressure fixed-bed reactor built

by Xiamen HanDe Engineering Co., Ltd. Typically, 0.50 g catalyst with grain sizes of 250-600 μm (30-60 meshes) was loaded in a titanium reactor (inner diameter, 10 mm). The ratio of height/diameter for the catalyst bed was approximately 1:1. The reactant with a H_2/CO_2 ratio of 3/1 and a pressure of 3.0 MPa was introduced into the reactor. Argon with a concentration of 8.0% in the H_2/CO_2 mixture was used as an internal standard for the calculation of CO_2 conversion. Before the reaction, the catalyst was pre-reduced with hydrogen at 400 $^\circ\text{C}$ for 3 h. Then, the temperature was raised to the desired reaction temperature (typically 370 $^\circ\text{C}$) to start the reaction. Products were analyzed by an online gas chromatograph, which was equipped with a thermal conductivity detector (TCD) and a flame ionization detector (FID). TDX-01 packed column was connected to TCD, while RT-Q-BOND-PLOT capillary column was connected to FID. The selectivity without CO was calculated on a molar carbon basis among products including hydrocarbons, methanol and dimethyl ether (DME). Carbon balances were all better than 95%. The catalytic performance after 10 h of reaction was typically used for discussion.

Catalyst characterization

X-ray powder diffraction (XRD) patterns were recorded on a Rigaku Ultima IV diffractometer. The diffraction angles were scanned from 10 to 80 degrees (2θ) with a speed of 10 degree min^{-1} . Cu $\text{K}\alpha$ radiation ($\lambda = 0.15406 \text{ nm}$) at 40 kV and 30 mA was used as the X-ray source.

Electron paramagnetic resonance (EPR) spectroscopic measurements were performed on a Bruker EMX-10/12 EPR spectrometer operated at X-band frequency. The parameters for EPR measurements were as follows: microwave frequency 9.5 GHz, microwave power 20 mW, modulation frequency 100 kHz, attenuator 10 dB. For the EPR measurements, 100 mg Zn–Ga–O powder was pre-reduced in H_2 at 400 $^\circ\text{C}$ for 3 h. Then, the sample was placed in a sealed glass tube. The sealed glass tube was placed in the microwave cavity for EPR measurements at $-196 \text{ }^\circ\text{C}$ under liquid nitrogen atmosphere. 1,1-Diphenyl-2-picryl-hydrazyl was used as an internal standard to quantify the intensity of EPR signals.

Scanning electron microscopy (SEM) measurements were performed on a Hitachi S-4800 operated at 15 kV. The sample was dispersed ultrasonically in ethanol for 10 min. Then, the suspension was dropped onto a silicon pellet and was dried for 1 h. Transmission electron microscopy (TEM) measurements were performed on a Phillips Analytical FEI Tecnai20 electron microscope operated at an acceleration voltage of 200 kV. The sample was dispersed ultrasonically in ethanol for 5 min, and a drop of solution was deposited onto a carbon-coated copper grid. More than 200 particles were used to estimate the mean particle size from TEM images.

H₂-Temperature-programmed reduction (H₂-TPR) measurements were performed on a home-made apparatus with a thermal conductivity detector (TCD) in a H₂-Ar mixture (5 vol.% H₂). Prior to reduction, the catalyst (100 mg) was pretreated in air flow at 400 °C for 2 h, and then cooled down to 50 °C. After that, H₂-TPR experiment was started by raising the temperature to 800 °C at a rate of 10 °C min⁻¹.

In situ Diffuse Reflection Infrared Fourier Transform Spectroscopy (DRIFTS) measurements were performed to characterize the reaction intermediates on ZnGa₂O₄ surfaces at ambient pressure (0.1 MPa). The spectra were performed on a Nicolet 6700 instrument equipped with an MCT detector. *In situ* absorbance spectra were obtained by collecting 120 scans at 8 cm⁻¹ resolution. Before measurement, catalyst was pre-reduced with a H₂ flow at 400 °C for 1 h, followed by purging with a 30 mL min⁻¹ N₂ for 30 min. Subsequently, the catalyst was cooled down to 370 °C. The background spectrum was obtained at 370 °C in N₂ flow. Catalyst was exposed to CO₂ for 60 min, followed by a 30 mL min⁻¹ N₂ flow for 30 min to sweep the gaseous CO₂. After that, H₂ with a flow rate of 30 mL min⁻¹ was introduced. The evolution of surface species was recorded at different times.

Supplementary tables and figures

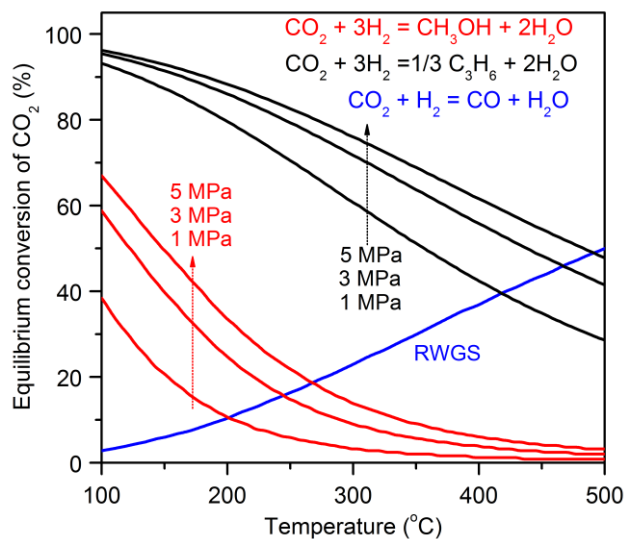


Fig. S1 Equilibrium conversions of CO₂ for the hydrogenation of CO₂ into methanol and propylene (a representative of lower olefins) as well as the RWGS reaction. Simulated conditions: H₂/CO₂ = 3. The calculation was based on HSC5 chemistry software.

The synthesis of propylene from CO₂ is more feasible than the synthesis of methanol at higher temperatures. The RWGS reaction is also thermodynamically more feasible at higher temperatures.

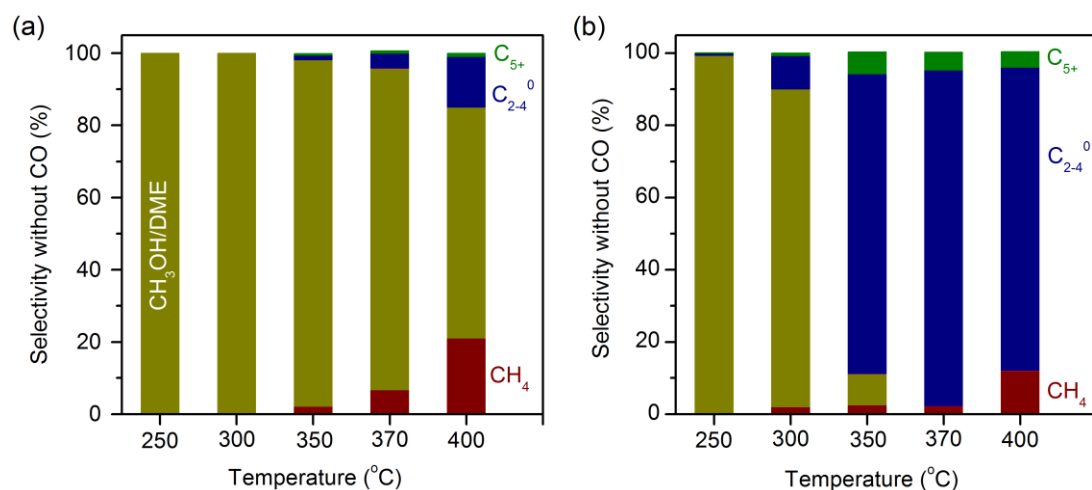


Fig. S2 Effect of reaction temperature on product distribution without CO. (a) Cu-Zn-Al oxide catalyst. (b) Cu-Zn-Al/SAPO-34 catalyst. Reaction conditions: $H_2/CO_2 = 3:1$, W (Cu-Zn-Al) = 0.17 g, W (Cu-Zn-Al/SAPO-34) = 0.50 g, time on stream 10 h, $P = 3$ MPa, $F = 45$ mL min^{-1} . The conversion of CO_2 and the selectivity of CO by the RWGS reaction were displayed in Table S1.

Table S1 Effect of reaction temperature on the conversion of CO₂ over Cu–Zn–Al oxide catalyst and Cu–Zn–Al/SAPO-34 catalyst.^a

Catalysts	Temp. (°C)	CO ₂ conv. (%)	CO select. (%)	Selectivity without CO (%)		
				C _m H _n ^b	CH ₃ OH	DME
Cu–Zn–Al	250	8.2	61	0	100	0
Cu–Zn–Al	300	19	88	0	100	0
Cu–Zn–Al	350	24	89	4.0	96	0
Cu–Zn–Al	370	28	94	11	89	0
Cu–Zn–Al	400	33	99	36	64	0
Cu–Zn–Al/SAPO-34	250	8.4	54	1.0	43	56
Cu–Zn–Al/SAPO-34	300	20	75	12	36	52
Cu–Zn–Al/SAPO-34	350	26	80	91.4	7.5	1.2
Cu–Zn–Al/SAPO-34	370	29	88	100	0	0
Cu–Zn–Al/SAPO-34	400	33	99	100	0	0

^a Reaction conditions: H₂/CO₂ = 3:1, *W*(Cu–Zn–Al) = 0.17 g, *W*(Cu–Zn–Al/SAPO-34) = 0.50 g, time on stream 10 h, *P* = 3 MPa, *F* = 45 mL min⁻¹.

^b Hydrocarbon products.

Table S2 Effect of reaction temperature on the conversion of CO₂ over ZnGa₂O₄ catalyst and ZnGa₂O₄/SAPO-34 catalysts.^a

Catalysts	Temp. (°C)	CO ₂ conv. (%)	CO select. (%)	Selectivity without CO (%)		
				C _m H _n	CH ₃ OH	DME
ZnGa ₂ O ₄	250	0.6	0	0	100	0
ZnGa ₂ O ₄	300	1.5	26	0	100	0
ZnGa ₂ O ₄	350	7.1	46	0	100	0
ZnGa ₂ O ₄	370	9.8	68	0.2	99.6	0.2
ZnGa ₂ O ₄	400	19	92	1.0	99	0
ZnGa ₂ O ₄	450	33	99	11	88.2	0.4
ZnGa ₂ O ₄ /SAPO-34	250	1.0	0	11	41	48
ZnGa ₂ O ₄ /SAPO-34	300	2.0	19	82	11	7
ZnGa ₂ O ₄ /SAPO-34	350	7.7	41	99.6	0.4	0
ZnGa ₂ O ₄ /SAPO-34	370	13	46	100	0	0
ZnGa ₂ O ₄ /SAPO-34	400	22	66	100	0	0
ZnGa ₂ O ₄ /SAPO-34	450	37	85	100	0	0

^a Reaction conditions: H₂/CO₂ = 3:1, $W(\text{ZnGa}_2\text{O}_4) = 0.17$ g, $W(\text{ZnGa}_2\text{O}_4/\text{SAPO-34}) = 0.50$ g, time on stream 10 h, $P = 3$ MPa, $F = 45$ mL min⁻¹.

Table S3 Effect of contact time on the conversion of CO₂ over ZnGa₂O₄/SAPO-34 catalyst.^a

<i>W/F</i> (s g mL ⁻¹)	CO ₂ conv. (%)	CO select. (%)	Selectivity without CO (%)		
			C _m H _n	CH ₃ OH	DME
0.05	2.1	29	73	21.3	5.7
0.1	3.8	36	94	5.2	0.8
0.2	6.0	40	98.6	1.3	0.1
0.4	9.4	42	99.4	0.6	0
0.7	13	46	100	0	0
1.0	14	57	100	0	0
1.2	16	64	100	0	0

^a Reaction conditions: H₂/CO₂ = 3:1, *W*(ZnGa₂O₄/SAPO-34) = 0.040-0.90 g, time on stream 10 h, *P* = 3 MPa, *T* = 370 °C, *F* = 45 mL min⁻¹.

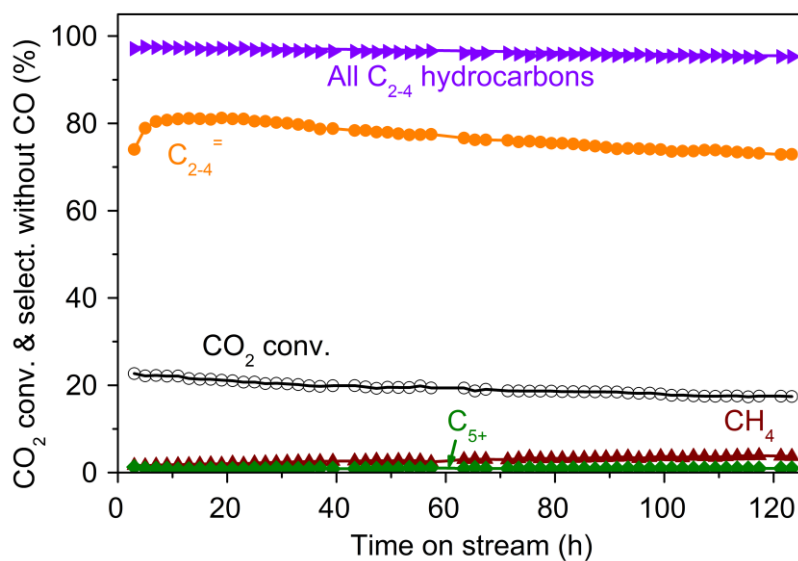


Fig. S3 Stability of the ZnGa₂O₄/SAPO-34 catalyst. Reaction conditions: H₂/CO₂ = 3:1, *W*(ZnGa₂O₄/SAPO-34) = 0.50 g, *T* = 400 °C, *P* = 3 MPa, *F* = 45 mL min⁻¹. The selectivity of CO by the RWGS reaction was in the range of 65-68%.

Table S4 Comparison of CO₂ and CO hydrogenation over ZnGa₂O₄ catalyst.^a

Reagent	CO ₂ conv. (%)	CO select. (%)	CO conv. (%)	CO ₂ select. (%)	Select. without CO or CO ₂ (%) ^b			CH ₃ OH/DME formation rate (mmol h ⁻¹ g ⁻¹)
					C _m H _n	CH ₃ OH	DME	
CO/H ₂	-	-	1.7	35	6.2	64	30	1.7
CO ₂ /H ₂	9.8	68	-	-	0.2	99.4	0.4	5.5

^a Reaction conditions: H₂/CO = 3:1 or H₂/CO₂ = 3:1, $W(\text{ZnGa}_2\text{O}_4) = 0.17$ g, time on stream 10 h, $P = 3$ MPa, $T = 370$ °C, $F = 45$ mL min⁻¹.

^b Selectivity among hydrocarbons, CH₃OH and DME.

Table S5 Effect of Zn/Ga ratio on the conversion of CO₂ over Zn–Ga–O and Zn–Ga–O/SAPO-34 catalysts.^a

Catalysts ^b	CO ₂ conv. (%)	CO select. (%)	Product select. (%)					
			CH ₄	C ₂₋₄ ⁼	C ₂₋₄ ⁰	C ₅₊	CH ₃ OH	DME
Ga ₂ O ₃	4.8	94	0.9	0	0	0	63.9	35.2
Zn–Ga–O (1:8)	6.0	87	0.6	0	0	0	59	40.4
Zn–Ga–O (1:4)	8.0	77	0.2	0	0	0	66.5	33.3
Zn–Ga–O (1:2)	9.8	68	0.2	0	0	0	99.4	0.3
Zn–Ga–O (1:1)	8.8	72	0.2	0	0	0	99.4	0.4
Zn–Ga–O (4:1)	5.3	86	0.2	0	0	0	99.3	0.5
ZnO	3.4	99.5	0.7	0	0	0	99.1	0.2
Ga ₂ O ₃ /SAPO-34	5.1	85	2.6	62	27	8.6	0	0
Zn–Ga–O (1:8)/SAPO-34	6.5	79	1.7	55	32	11	0	0
Zn–Ga–O (1:4)/SAPO-34	8.8	68	0.9	66	28	5.5	0.2	0.02
Zn–Ga–O (1:2)/SAPO-34	13	46	1.0	86	11	2.0	0	0
Zn–Ga–O (1:1)/SAPO-34	11	49	2.3	82	14	2.0	0	0
Zn–Ga–O (4:1)/SAPO-34	6.0	78	3.5	63	30	4.0	0	0
ZnO/SAPO-34	3.8	99	10	59	26	5.1	0	0

^a Reaction conditions: H₂/CO₂ = 3:1, $W(\text{Zn–Ga–O}) = 0.17$ g, $W(\text{Zn–Ga–O/SAPO-34}) = 0.50$ g, time on stream 10 h, $P = 3$ MPa, $T = 370$ °C, $F = 45$ mL min⁻¹. Selectivity was calculated on molar carbon basis among the products including hydrocarbons, CH₃OH and DME. The selectivity of CO was calculated separately.

^b The number in the parenthesis denotes the Zn/Ga ratio.

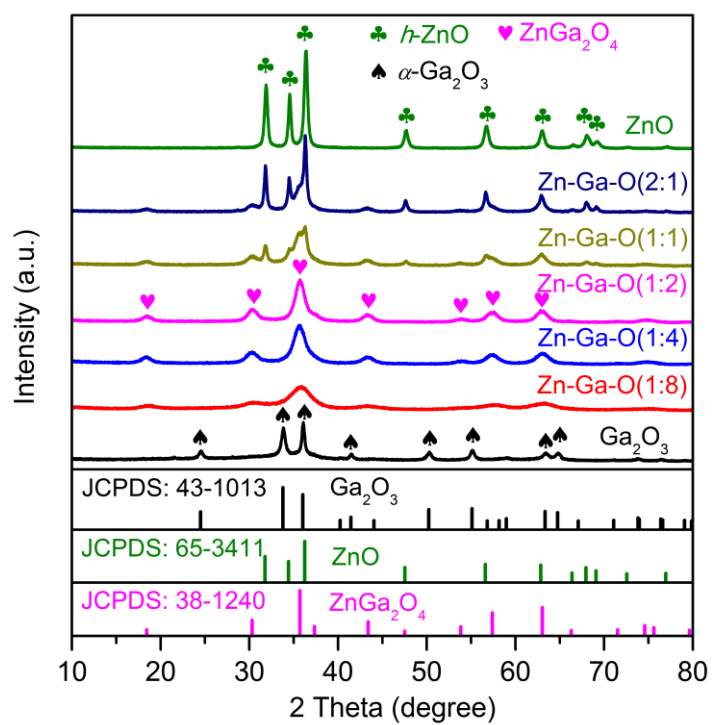


Fig. S4 XRD patterns of Zn–Ga–O catalysts with different Zn/Ga ratios as well as ZnO and Ga₂O₃.

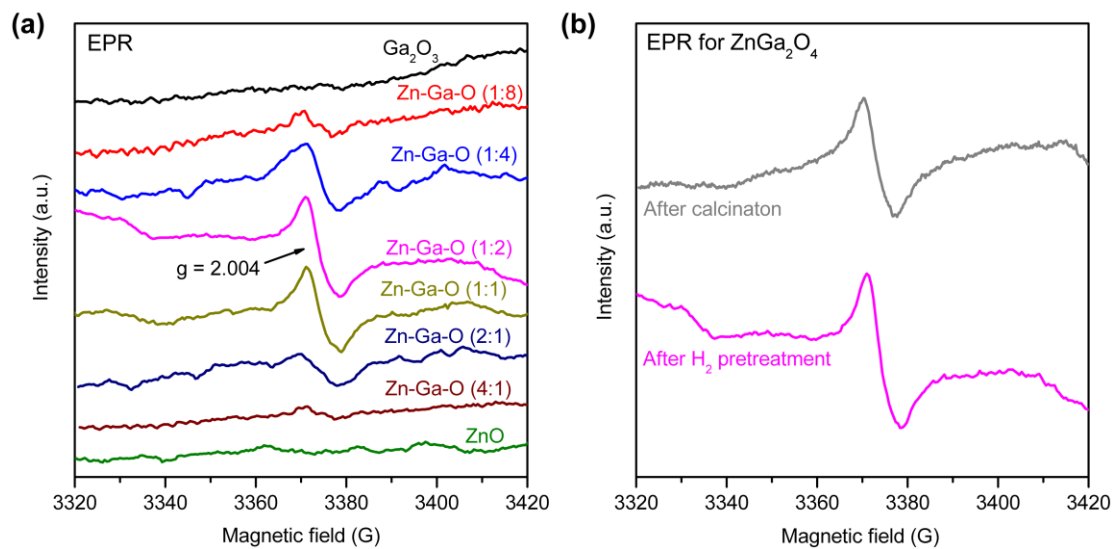


Fig. S5 (a) EPR spectra for Zn–Ga–O catalysts with different Zn/Ga ratios as well as ZnO and Ga₂O₃ after pretreatment by H₂. (b) EPR spectra for ZnGa₂O₄ catalyst after calcination and after pretreatment by H₂.

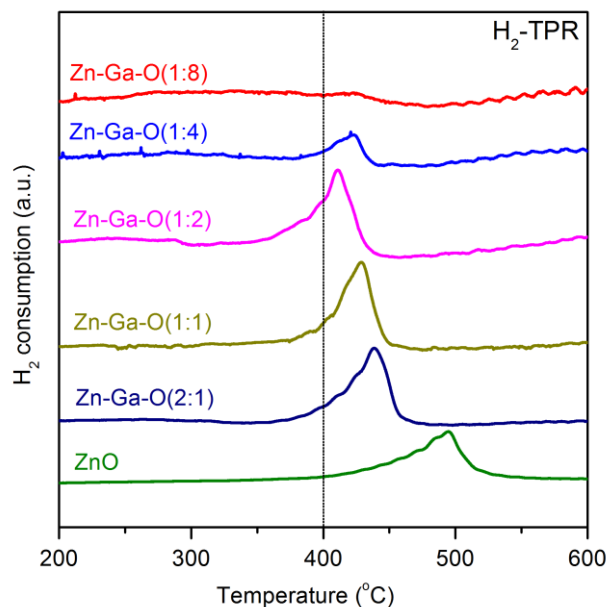


Fig. S6 H₂-TPR profiles for Zn–Ga–O catalysts with different Zn/Ga ratios as well as ZnO and Ga₂O₃.

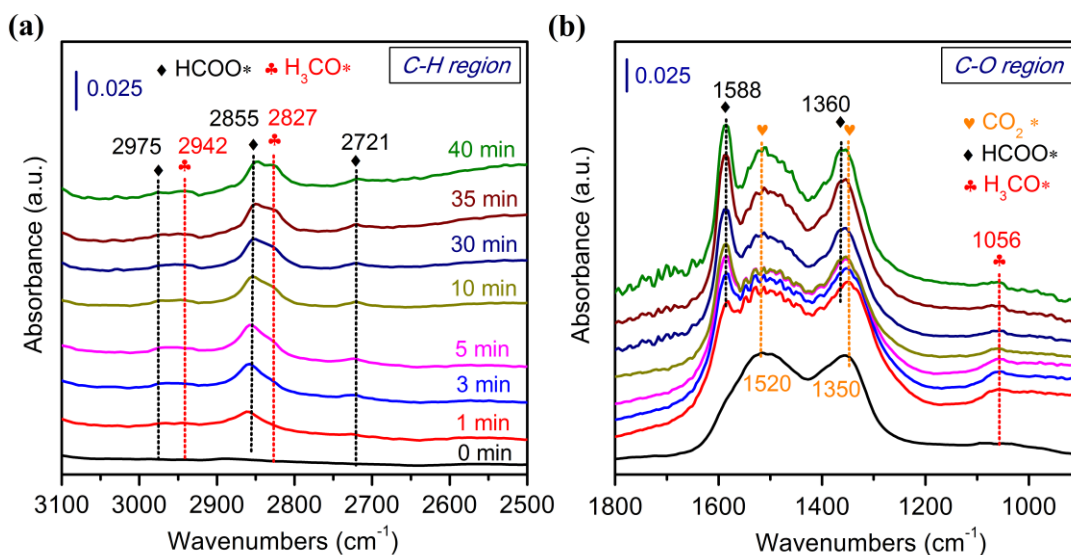


Fig. S7 *In situ* DRIFT spectra for the ($\text{CO}_2 + \text{H}_2$) reaction on ZnGa_2O_4 catalyst. (a) 3100–2500 cm^{-1} . (b) 1800–1000 cm^{-1} . The sample was reduced *in situ* at 400 °C for 1 h. Before CO_2 adsorption, gaseous and weakly absorbed H_2 molecules were purged by N_2 flow. The adsorption of CO_2 was conducted at 370 °C for 1 h. Then, a flow of H_2 was introduced.

The bands at around 1520 cm^{-1} [$\nu_{\text{as}}(\text{OCO})$] and 1350 cm^{-1} [$\nu_{\text{s}}(\text{OCO})$] can be attributed to absorbed CO_2 species on oxygen vacancies and carbonate species.² The bands at 2975 cm^{-1} [$\delta(\text{CH}) + \nu_{\text{as}}(\text{OCO})$], 2855 cm^{-1} [$\nu(\text{CH})$], 2721 cm^{-1} [$\delta(\text{CH}) + \nu_{\text{s}}(\text{OCO})$], 1588 cm^{-1} [$\nu_{\text{as}}(\text{OCO})$] and 1360 cm^{-1} [$\nu_{\text{s}}(\text{OCO})$] are attributable to formate species.²⁻⁴ The bands at 2942 cm^{-1} [$\nu_{\text{as}}(\text{CH}_3)$], 2827 cm^{-1} [$\nu_{\text{s}}(\text{CH}_3)$] and 1056 cm^{-1} [$\nu(\text{CO})$ of terminal (t-OCH₃)] can be attributed to methoxide species.⁴

References

- 1 L. Xu, A. Du, Y. Wei, Y. Wang, Z. Yu, Y. He, X. Zhang and Z. Liu, *Micropor. Mesopor. Mater.*, 2008, **115**, 332–337.
- 2 (a) A. M. Turek, I. E. Wachs and E. DeCanio, *J. Phys. Chem.*, 1992, **96**, 5000–5007; (b) J. I. Di Cosimo, V. K. Díez, M. Xu, E. Iglesia and C. R. Apesteguía, *J. Catal.*, 1998, **178**, 499–510; (c) L. Liu, C. Zhao and Y. Li, *J. Phys. Chem. C*, 2012, **116**, 7904–7912.
- 3 (a) K. K. Bando, K. Sayama, H. Kusama, K. Okabe and H. Arakawa, *Appl. Catal. A*, 1997, **165**, 391–409; (b) W. O. Gordon, Y. Xu, D. R. Mullins and S. H. Overbury, *Phys. Chem. Chem. Phys.*, 2009, **11**, 11171–11183.
- 4 (a) S. Kattel, B. Yan, Y. Yang, J. G. Chen and P. Liu, *J. Am. Chem. Soc.*, 2016, **138**, 12440–12450; (b) K. Larmier, W. C. Liao, S. Tada, E. Lam, R. Verel, A. Bansode, A. Urakawa, A. Comas-Vives and C. Copéret, *Angew. Chem. Int. Ed.*, 2017, **56**, 2318–2323.